Advancements in Monofilament Structural Composite Technology

W. J. Crichlow* and V. S. Sorenson†
Lockheed-California Company, Burbank, Calif.

This paper describes recent studies of large-diameter (0.003–0.005 diam) "S"-glass filaments for use in primary load-bearing aircraft structure. Unidirectional composite average compressive strengths of 192,000 psi and average tensile strengths of 109,000 psi were recorded. Filament compressive stresses over 400,000 psi and tensile stresses over 350,000 psi were obtained in cross-laminated composites. The developed technology, covering materials, and design and fabrication were demonstrated by constructing and testing coupons and two wing box beams. Results of static and fatigue tests are reported.

Introduction

THERE is a wide gap between basic materials research and practical engineering application of fibrous composites. Although virgin glass-fiber strength properties always have been relatively high, glass-fiber reinforced composites have been plagued with two major deficiencies: low effective modulus and low strength-to-weight ratios.

Effective utilization of high tensile properties of glass filaments has been made in rocket motor cases and high pressure vessels. These structures are unique in two respects: 1) they have an ideal shape (cylindrical or spherical) that readily lends itself to filament-winding techniques; and 2) loading conditions (generally simple membrane tensions) are ideal, which makes most effective use of the filamentary properties. Airframe structure, unfortunately, is unaccommodatingly complex in shape, and is subject to all possible combinations of stresses: tensile, compressive, shear, bending, etc. It must be safely man-rated, and should last indefinitely under repeated usage.

Since normal factory handling of a single-strand brittle material is patently impractical, a research program was initiated to devise and demonstrate a practical and complete materials handling system for making monofilament structural composites. *S*-glass filament material of 0.003 to 0.005 in. diam (approximately ten times the size of normal glass fiber) was selected, and a high viscosity epoxy resin was chosen as the transport material. The *S*-glass filament, formed at the furnace bushing, immediately was coated with HTS finish and wound with controlled spacing into a single layer on a cylinder and bound together with the epoxy resin. Cutting the glass-filament-covered resin-paper film from the winding drum results in an intermediate pre-preg sheet product of unidirectional parallel-oriented monofilament. Composite laminates are made by stack-laying any number of sheets in the required filament orientation, and pressure curing. This paper presents data for static and fatigue strengths of laminated composite sheets of material made by this process, and describes the construction and static test of a sandwich panel wing box beam designed to demonstrate the process.

Design Properties

The properties of composites are illustrated in the shaded area of Fig. 1, which compares strength/density ratios and stiffness/density ratios of filaments and several composites made of these filaments with conventional structural metals.[1] This diagram illustrates clearly a strength-density superiority of certain configurations of *S*-glass laminates. However, the stiffness-density ratio is restricted severely by the low modulus of the glass filaments. For stiffness-critical structures, the marked superiority of composites of the advanced filament is clear. Aeroelastic or compression stability-critical structures will derive the greatest benefits from increased stiffness/weight ratio.

An important quality of a successful structural material is its capability to absorb energy. This quality may be examined by considering the total energy absorbed per unit volume of material to fracture a structural element, as measured by the area under the stress-strain curve. Figure 2 shows a scale comparison of the stress-strain curves typical of several filaments and isotropic structural metals, along with *S*-glass and boron epoxy-filament composites. The problems of designing damage-tolerant and "forgiving" structures is somewhat in inverse ratio to the energy-absorbing capability of the material. Therefore, extreme care will be required in the design, fabrication, and in-service protection of structures made of the new advanced filaments.

Composite Geometry

Earlier work based on composites made from 0.003-in.-diam steel music wire-epoxy-polyurethane resin composites provided data on the geometrical relation of filaments and resins applicable to composites made from large-diameter glass or high-modulus filaments.[2] These results indicated an optimum filament diameter to spacing ratio, approximately 0.80, and that alternating adjacent layers provided maximum compressive properties.

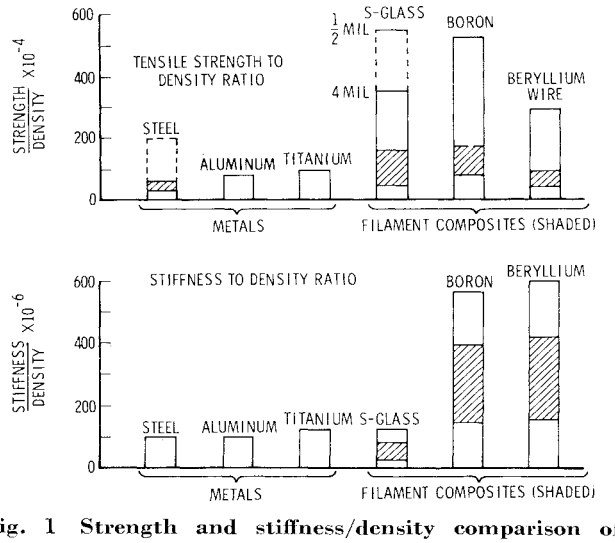

Fig. 1 Strength and stiffness/density comparison of composites and metals.

Presented as Preprint 65-761 at the AIAA/RAeS/JSASS Aircraft Design and Technology Meeting, Los Angeles, Calif., November 15–17, 1965; submitted December 9, 1965; revision received May 4, 1966.

* Group Research and Development Engineer, Advanced Materials and Structural Methods Department. Member AIAA.

† Senior Research Specialist, Materials and Processes Engineering Group.

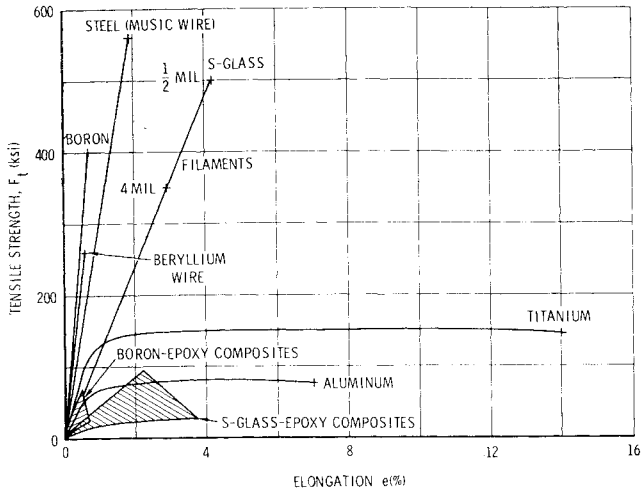

Fig. 2 Comparison and stress-strain curves for filaments, composites, and metals.

Composites utilizing high-modulus, high-strength, and low-density filaments show the most promising potential for a wide range of the loading index for composite sandwich construction. If the elastic properties of the material are known, it is possible to plot a curve of maximum attainable compressive buckling strength for plate elements as a function of the plate geometry and loading. The latter two quantities are expressed by the structural loading index N_x/b, where N_x is the load per inch width and b is the plate width. Curves of maximum compression buckling strength are shown in Fig. 3 for boron and S-glass filament composites in solid plate and honeycomb sandwich compared with aluminum alloy sheet and sandwich. It is significant that, except for a very high loading index, the composite is more efficient when used for faces in sandwich construction than the solid composite sheet, and, furthermore, in this low load-intensity range, filament composites have the potential of being more efficient than the best metals, with the possible exception of beryllium. However, final judgment of weight efficiency must include joint material, substructure and secondary material, and such other factors as reliability, inspectability, fatigue, and fail-safe design considerations.

Design Data Tests

To obtain design data on composite materials made from large-diameter S-glass filaments and epoxy resin, a number of laminates were fabricated. Basically the laminates were of

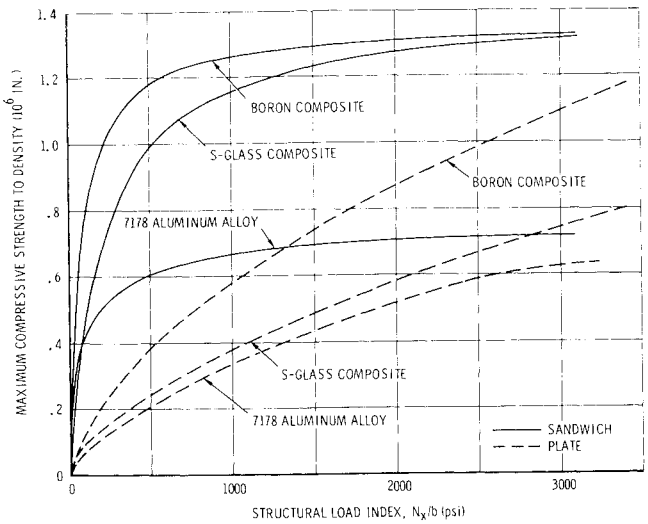

Fig. 3 Maximum compression strength/density vs structural load index.

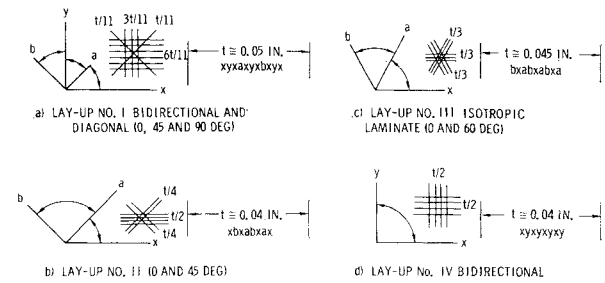

Fig. 4 Test laminate lay-up configurations.

four lay-up configurations, as shown in Fig. 4. Supplementary unidirectional and multidirectional laminates also were fabricated to provide additional information.

Interlaminar Shear Tests

Three-point, short beam flexural tests were conducted on coupons cut from 27-layer unidirectional composites. One set of coupons was made from epoxy resin and the second set was made from epoxy resin filled with 20% volume of chopped 0.3-mil-diam fibers. The interlaminar shear strength of the unfilled and filled resin system was 14,620 and 14,380 psi, respectively. Photomicrographs of the laminates showed that the chopped fibers were not oriented randomly, and no improvement in interlaminar shear strength was obtained.

Tension and Compression Coupon Tests

Results of the tensile and compressive tests are summarized in Table 1. The relation between filament stress, composite stress, and percent volume filaments in the loading direction is shown in Fig. 5. As shown, the composite stress is directly proportional to the percentage of filaments in the loading direction.

The filament stresses were determined by multiplying the measured strain by the modulus of elasticity of the filaments (12×10^6 psi) except as noted in Table 1. The filament stresses decrease as the percentage of filaments increases. The laminates used in the box beam are closer to Lay-up II. As shown in Table 1, both the tensile and compressive filament stresses were in excess of 300,000 psi for Lay-up II.

Fatigue Tests

Three types of fatigue tests were performed on hole-notched fatigue specimens cut from the S-glass composite laminates: constant amplitude S-N data, block spectra loading, and flight-by-flight spectra loading.

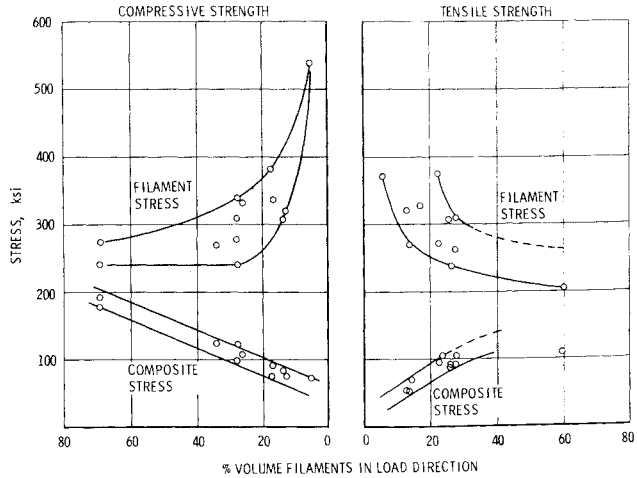

Fig. 5 Relation between strength and percent volume filaments in load direction.

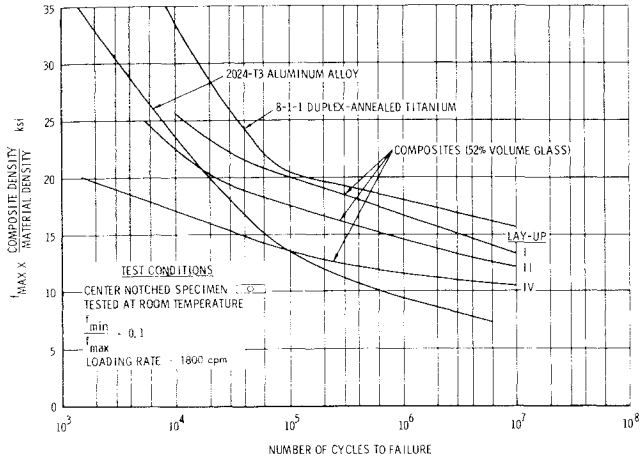

Fig. 6 Comparison of *S-N* curves for metals and large-diameter *S*-glass epoxy composites.

Constant amplitude S-N tests

Results of the conventional axial load *S-N* fatigue tests are given in Fig. 6. These tests were conducted at ambient temperature, under a loading rate of 1800 cycles per minute, and a stress ratio $R = f_{min}/f_{max} = 0.1$. Comparison of the test results for large-diameter *S*-glass composite laminates with those of equal weight of aluminum (2024-T3) and titanium (8Al-1Mo-1V) duplex-annealed sheet also is shown in Fig. 6. These curves indicate superior fatigue results for these composite materials in the low stress-high cycle range and equal or inferior results compared with 2024-T3 aluminum alloy sheet for the high stress-low cycle range. The titanium 8Al-1Mo-1V duplex-annealed sheet is superior in all stress ranges to these composites.

Spectrum fatigue tests

The inadequacy of *S-N* fatigue data to represent reliable fatigue results in variable loading environment is now well established. For this reason it has been the practice for many years to conduct spectrum fatigue tests in which all expected load levels are applied to the same material coupons. Fatigue test results are dependent upon the manner of blocking the random load spectrum into load groups of varying amplitude levels. Each group of loads is applied at an appropriate mean load level representing ground taxi mean loads, and flight mean load.

Perhaps the most sensitive fatigue cycle in block spectra is represented by the load excursion once per flight or ground-air-ground cycles. For example, the mean load transition from ground-air-ground is often chosen. Each flight, however, encounters some higher maximum excursion in flight and greater minimum excursion on the ground. To avoid these arbitrary decisions in the definition of the block loading spectra, it is also the practice to conduct spectrum fatigue tests on a flight-by-flight basis. This means ground taxi varying loads for each flight are applied at the ground-supported mean load level, flight varying loads per flight at flight mean load level, the cycle repeated on a per flight basis. Specific definition of a ground-air-ground transition cycle is avoided.

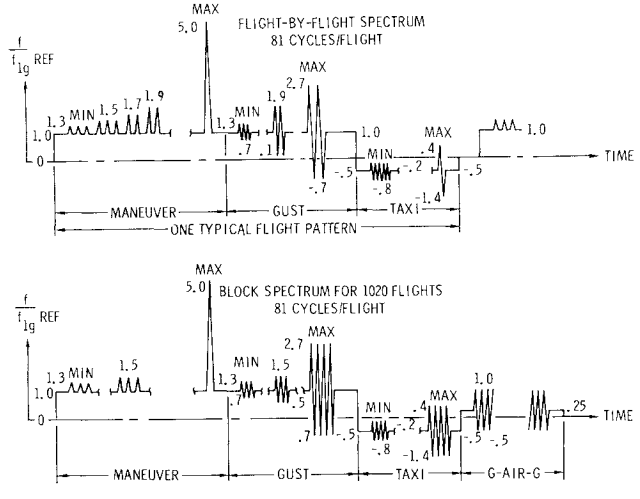

Fig. 7 Fatigue load spectrum for fighter wing.

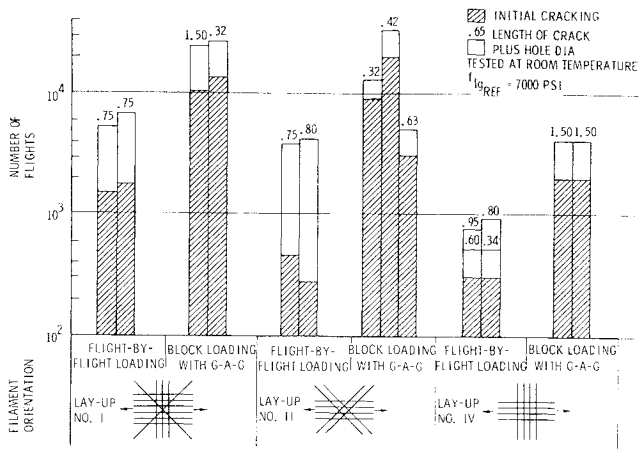

Fig. 8 Comparison of spectrum fatigue test results.

Spectrum testing, however, does have to be tailored to specific types of vehicles. A V/STOL fighter-type machine was of interest so a fighter spectrum related to MIL-A-8866 was constructed and put onto magnetic tape in two forms: 1) the block-ordered spectrum with ground-air-ground cycle defined as the mean load transition, and 2) the flight-by-flight sequence. The peak loads exceeding the once per flight level were interspersed uniformly among the flights. The schematic diagrams of the loading sequences are shown in Fig. 7. A magnetic tape-controlled electrohydraulic servo jack fatigue machine applies the desired sequence to the specimens.

The block spectrum and flight-by-flight test results are compared in Fig. 8. The flight-by-flight loading is more conservative. This result is consistent with similar experiments in metals. Of interest is the number of flights between discovery of the fatigue crack and final failure or termination of the tests. The rate of crack growth in these experiments was sufficiently low to expect good performance from the standpoint of ample inspection intervals and good residual static strength in the presence of fatigue cracks or other damage. The fail-safe nature of this material, of course, must be explored in much more detail.

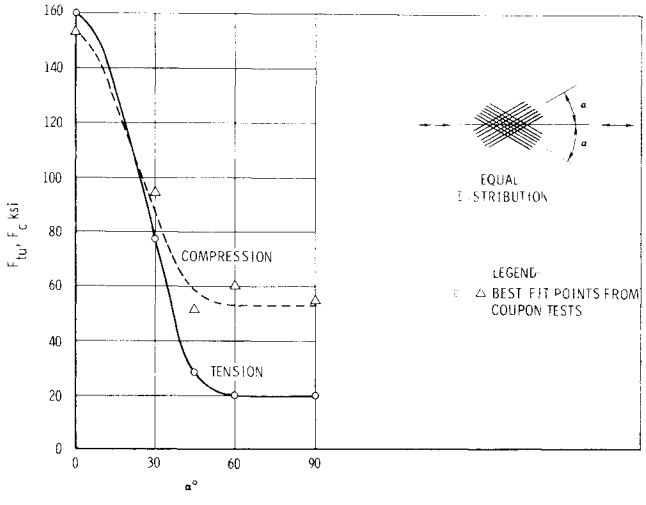

Fig. 9 Tension and compression strength vs lay-up angle.

Table I Summary of coupon test data (average of three coupons)

Laminate no.	Lay-up configuration	Load direction (deg)	% volume filaments	Tensile Strength: Gross area stress (psi)	Tensile Strength: Filament stress (psi)	Compressive Strength: Gross area stress (psi)	Compressive Strength: Filament stress (psi)
		0	...	97,300	272,000	96,900	240,000
I	Ref. Fig. 7	45	50.3	53,300	270,000	80,800	307,000
		90	...	35,900	366,000	70,700	540,000
		0	...	93,100	308,000	107,100	333,000
II	Ref. Fig. 7	45	52.0	54,600	321,000	76,800	319,000
		90	...	27,300	...	51,900	...
		0	...	66,200	329,000	91,100	337,000
III	Ref. Fig. 7	45	50.8	54,200	...	82,200	...
		90	...	58,600	...	81,300	...
		0	...	90,800	263,000[a]	120,000	309,000
IV A	Ref. Fig. 7	45	55.0	31,300	...	32,200	...
		90	...	104,000	311,000	97,500	277,000
IV D	Ref. Fig. 7	0	52.2	86,700	239,000	...	...
V A	5-0°/2−±45°/4-90°	0	50.0	102,400	372,000	...	...
1	8-0°/8-90°	0	37.5	...	...	71,300	382,000
14	11 layers @ 0°	0	69.0	...	...	177,000	240,000
17	Lay-up I	0	50.0	...	...	98,800	340,000
20	11 layers @ 0°	0	68.7	...	...	192,300	273,000
21	Lay-up I	0	62.0	...	...	124,000	269,600
24	11 layers @ 0°	0	59.5	109,300	202,000	138,000	232,000

[a] Calculated by deducting load carried by tranverse layers.

Determination of Design Allowables

To determine design allowables from test data obtained on a limited number of specific lay-ups, a method was established by which these data were translated into allowables for lay-ups having different filament orientations and layer distributions. This method was based on the concept of the "rule of mixtures," in which the ultimate strength for any lay-up can be described by the equation:

$$F_{\text{lay-up}} = \Sigma F_\alpha t_\alpha / \Sigma t_\alpha \quad (1)$$

where

α = angle between any one filament direction and the load axis
t_α = thickness of layer with filament in direction α
F_α = allowable stress for layer with filaments in direction α

To determine the function F_α in terms of α, the equation first is solved backwards for a number of values of α using test values of $F_{\text{lay-up}}$.

To do so, it is necessary to establish a set of equations

$$[t_{\alpha_{ij}}] \{F_{\alpha_j}\} = \{F_{\text{lay-up}_i}\} \quad (2)$$

The lay-ups tested must contain only orientations α_2 (not necessarily all in each lay-up) and no other, and a sufficient number of test results, i.e., of combinations of lay-ups and load-axis directions, must be available to form at least as many equations as the number of directions α_j. If more test measurements than directions are available, best-fit methods can be applied.

This approach was used to determine values F_α for α = 0°, 30°, 45°, 60°, and 90° using seven sets of measurements. The computed values of F_α were plotted in Fig. 9 for tension and compression. These curves were used to evaluate allowable stresses for other lay-ups, including those for the box beam.

The curves of Fig. 9 were computed for pairs of layers symmetrically oriented with respect to the load. If they are assumed applicable to single layers as well, they can be used to evaluate lay-ups that are not symmetrical with respect to the load axis. This procedure was applied to Lay-up III, loaded at an angle of 15° with respect to the x direction, for which test data were available, with the following results: tension tests averaged 90% of computed values, and compressive tests 104% of computed values.

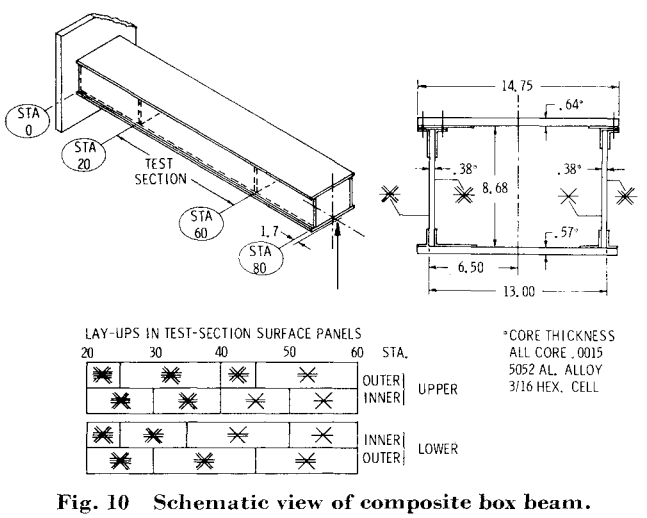

Fig. 10 Schematic view of composite box beam.

Design of the Box Beam

The design features of the box beam are summarized below.

Type: Cantilever, single-cell (two-spar) box, dimensioned as shown in Fig. 10.

Surfaces: Upper and lower surface, spars, and end-ribs were of honeycomb sandwich design. Faces were of laminated large-diameter glass layers, varying in thickness from 0.036 (eight layers) to 0.0135 in. (three layers). Three-sixteenth-in. hexagonal-cell honeycomb core of 5052 aluminum alloy, 0.0015-in.-thick foil (4.4 lb/ft^3) was used throughout, chosen for maximum stiffness-weight ratio. The upper surface was removable, attached by $\frac{3}{16}$-in.-diam screws. Aluminum powder-loaded resin was cast in place at each screw location to enhance bearing and crushing strengths.

Joints: With the exception of the upper surface attachments, all joints were adhesive bonded. Connecting angles and doublers were of laminated 181 S-glass fabric, with fibers generally oriented at ±45° with respect to the axis of the box for maximum shear strength.

Adhesives: Epoxy-polyamide film adhesives were selected for all adhesive-bonded joints including sandwich face-to-core bonds.

In lieu of statistical data, design allowable stresses were reduced 75% of average coupon data to allow for variations of material properties.

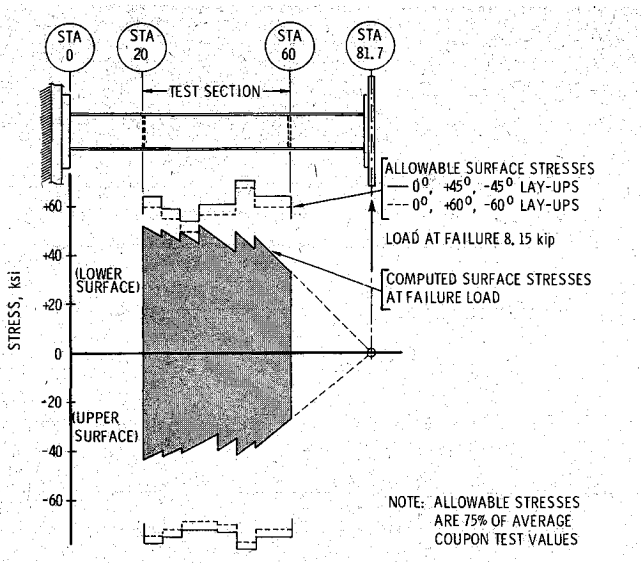

Fig. 11 Allowable and computed stresses for box surfaces.

Static Test of Box Beam

The box specimen was loaded as a cantilever beam, as shown schematically in Fig. 10. One end of the box beam was attached to a test head through high-strength structural steel fittings. Loads were applied to the free end through similar steel fittings. The load was applied by hydraulic jacks located on the centerline.

Two tests were conducted. First, the beam was loaded in increments to 5160 lb in symmetrical down-bending. In the second, the box was loaded in increments in the symmetrical up-bending condition. At 8150 lb the lower surface (tension cover) failed. The rear spar at Station 20 also failed, in a secondary rupture.

The failure of the tension cover occurred between Stations 52.5 and 56. Separation occurred between the tension cover and the spar caps because of delamination of the inside skin. Inspection of the failure revealed that plies of the inside tension cover could be peeled apart easily, thus indicating poor interlaminar bond. The resin in the failed region was finely cracked over an extensive area giving it a loose granular sugar-crystal appearance. In addition, it was found that the $\pm 45°$ shear layers had been made laid up at $\pm 60°$ to the longitudinal axis of the box through a fabrication error.

Referring to Fig. 11, it is seen that the failure did not occur in the part of the box beam indicated most critical by analysis. The tension surface between Stations 30 and 35 is the most critical region since the strength margin at failure load was zero at this location. In the failure area, between Stations 52.5 and 56, the computed stresses were from 38,600 to 43,900 psi. On the basis of the average coupon data (80,000 psi), the reduced design allowable strength is 60,000 psi. The test stresses were well below this value.

One factor investigated was the possibility of overcuring. To determine the effect of the extended cure cycles, unidirectional laminates of 22 layers were subjected to various cure cycles. Interlaminar shear tests (Table 2) indicate the shear strength of the resin was not affected by the six cure cycles

Table 2 Summary of flexural tests

No. of cure cycles	Average interlaminar shear strength (psi)
1 hr at 350°F and 1 hr at 250°F	14,625
2 times at 350°F for 1 hr and 2 times at 250°F for 1 hr	14,500
3 times at 350°F for 1 hr and 3 times at 250°F for 1 hr	14,650
4 times at 350°F for 1 hr and 4 times at 250°F for 1 hr	13,850

Table 3 Sandwich compression coupon tests

Lay-up Configuration in Each Face	Compressive Strength (psi) Inside Surface	Outside Surface
60° 60°	41,000	41,000
60° 60°	26,500	59,600
60° 60°	38,900	59,000

Table 4 Tensile coupon tests

Coupon No.	Lay-up Configuration		Gross Area Stress (psi)	Filament Stress (psi)
B1T1	60° 60°	Outside Skin	79,400	322,000
B1T2			76,400	343,000
B1T3			77,100	340,000
Avg			77,600	335,000
B1T4	60° 60°	Inside Skin	49,500	179,000
B1T5			50,000	181,000
B1T6			56,000	205,000
Avg			51,800	188,000

used for the box beam. Eight cure cycles lowered the interlaminar shear strength about 6%. Therefore, the failure cannot be attributed entirely to reduction in strength due to overcuring.

Compression and tension test coupons were cut from unfailed skin material near the failure zone. Results of these tests (Tables 3 and 4) indicate the inside skin to be approximately two-thirds the strength of the exterior skin for the same lay-up configuration. The skin delamination mode of failure in these tests indicated poor binding strength of the resin.

The box beam applied stress at the analysis critical Station 35 is covered adequately by the 51,800 psi strength of the inside skin at this point. However, the estimated strength of 40,000 psi for the configuration at the failure station is marginal for the test applied stresses of 43,900 psi at Station 52.5 and 38,100 psi at Station 56. Therefore, the failure can be attributed to the low strength of the laminate on the inside surface in the failure area.

Summary and Conclusions

The results of a development program to establish fabrication techniques and design data for utilizing large-diameter S-glass fibers and epoxy-resin composites in primary airframe structures indicate that for compression applications these composite materials show considerable advantage on a strength/density basis over currently available composite and metallic materials. The tensile strength, on the other hand, is about two-thirds the strength of conventional filament-wound glass-epoxy composites. The fatigue properties are comparable to those of metals in the low stress-high cycle range. Flight-by-flight spectrum fatigue tests on notched-hole coupons indicate that these materials have a slow crack-growth rate. Demonstration of practical processing and fabrication techniques for production of filament composite primary structure has been achieved. However, considerable development work remains to produce a consistent product and fly a man-rated aircraft of filament-composite primary structure.

References

[1] Yaffee, M. L., "Composite materials offer vast potential for structures," Aviation Week and Space Technology (May 3, 1965).

[2] Ekvall, J. C., "Elastic properties of orthotropic monofilament laminates," ASME Paper 61-AV-56 (March 12–16, 1961).